



Behaviour of TEM metal-grids during *in-situ* heating experiments

Z. Zhang, D.-S. Su

, Departement of Inorganic Chemistry, Fritz-Haber-Institut of the Max-Planck-Gesellschaft,
D-14195 Berlin, Germany

Received 31 January 2007; revised 5 January 2009; accepted 28 January 2009. Available online 13 February 2009

Abstract

The stability of Ni, Cu, Mo and Au TEM grids coated with ultra-thin amorphous carbon or silicon monoxide film is examined by *in-situ* heating up to a temperature in the range 500–850 °C in a transmission electron microscope. It is demonstrated that some grids can generate nano-particles either due to the surface diffusion of metal atoms on amorphous film or due to metal evaporation/redeposition. The emergence of nano-particles can complicate experimental observations, particularly in *in-situ* heating studies of dynamic behaviours of nanomaterials in TEM. The most widely used Cu grid covered with amorphous carbon is unstable, and numerous Cu nano-particles start to form once heating temperature reaches 600 °C. In the case of Ni grid covered with α -C film, a large number of Ni nano-crystals occur immediately when the temperature approaches to 600 °C, accompanied by the graphitization of amorphous carbon. In contrast, both Mo and Au grids covered with α -C film exhibit good stability at elevated temperature, for instance, up to 680 °C and 850 °C for Mo and Au, respectively, and no any metal nano-particles are detected. Cu grid covered Si monoxide thin film is stable up to 550 °C, but Si nano-crystals appear under intensive electron beam. The generated nano-particles are well characterized by spectroscopic techniques (EDXS/EELS) and high-resolution TEM. The mechanism of nano-particle formation is addressed based on the interactions between the metal grid and the amorphous carbon film and on the sublimation of metal.

Keywords: *In-situ* TEM; Metal grid; Nano-particles; Carbon film; HRTEM; EELS

1. Introduction

There is remarkable research interest in nano-particles as they exhibit unique physical and chemical properties due to their small size [1-2]. Great effort has been made to explore and to understand the relationships between the size and the microstructure and the various properties of the nano-particles. The transmission electron microscope (TEM) is a most suitable and powerful tool for revealing the structure and surface states of nano-particles on an atomic scale, and for deducing correlations between microstructures and their properties [2]. With modern TEMs, the chemical information and structural characteristics of single nano-particle can be fully revealed. The dynamic behaviour in phase transformations, atomic arrangements, and mobility as well as sintering behaviour of nano-particles at high temperature are usually studied *in-situ* in high-resolution TEM (HRTEM) or in conventional TEM [3]. Such *in-situ* experiments are particularly important for understanding the mechanism of specific catalytic

behaviour of nano-particles, in which a correlation between catalytic performance and microstructure of nano-particles under a certain gas atmosphere must be established.

Recently, *in-situ* heating experiments have shown that nano-materials can be welded within TEM [4]; they can undergo changes in shape and structure (structural fluctuations) [5]. A variation of thermal wetting behaviour of Pt nano-particles on different substrates was reported [6]. The surface diffusion and coalescence of mobile metal nano-particles during *in-situ* heating treatment have been closely examined at atomic level indicating that a liquid-like surface layer of the nano-particles plays an essential role in this process [7]. Obviously, *in-situ* TEM heating is an important method for probing the unique properties of nano-materials at high temperature and the structure evolution at atomic resolution.

So far, in most *in-situ* heating experiments the nano-particles are dispersed on the ultra-thin amorphous carbon (α -C) or silicon monoxide films, which is mounted on a Cu grid [4, 8] or Ni [9], Mo [10] grid. However, there is no

systematic investigation of the stability of such metal grids at high temperatures in high vacuum. It is unclear whether such grids with thin film on it are affected chemically or structurally during heating and thus influence the experimental results of *in-situ* heating. Up to now, only a few publications point out that at elevated temperature Cu grid can evaporate in TEM column at 820°C, leading to the formation of Cu nano-rods and nano-particles on the α -C film [11].

In this work, we have studied the behaviour of TEM grids used for *in-situ* heating experiment to get a general overview of the stability and possible influence of TEM grids in the experimental observation at elevated temperature. A series of experiments using only TEM grids (Ni, Cu, Mo, and Au grids) were performed to explore the formation of nano-crystals on the support films during *in-situ* heating up to 850°C and to characterize these nano-crystals using electron energy-loss spectroscopy (EELS), energy-dispersive X-ray spectroscopy (EDXS) and high-resolution TEM (HRTEM). Furthermore, general suggestions are given for TEM *in-situ* heating experiments.

2. Experimental procedures

The microscope used in this study is a Philips CM200 FEG (field-emission gun) with a super-twin objective lens, equipped with a Gatan Tridiem Image Filter system for EELS measurement and an energy dispersive X-ray detector (Si -Li detector) for compositional analysis. The point resolution is 0.18nm (Cs = 1.35 mm, Scherzer defocus) when operated at an acceleration voltage of 200 kV. All images are recorded with a Gatan CCD camera (2048 pixels \times 2048 pixels). Some heating experiments were performed in a Philips CM200 LaB6 microscope (under Scherzer defocus, the point resolution 0.23 nm), working at 200 kV. A Gatan double tilt-heating holder (Model 652-Ta) is used for *in-situ* heating; the temperature was measured by using a thermocouple attached to the furnace [12]. The maximum operating temperature for this holder is up to 1000°C. During heating experiments, the electron beam is switched off to avoid the irradiation effect. Both EELS and EDXS spectra were performed in this microscope. EELS spectra were acquired in image mode with a dispersion of 0.5eV/channel. Acquisition times for low-loss and core-loss spectra are 0.1 s and 2~10 s, respectively. EELS spectra were processed using Digital Micrograph and EL/P software. A power law function and the Hartree-Slater model were used to remove the background and to quantify the compositions. For EDXS spectra, the acquisition time is usually set to 100 s.

The α -C films on metal grids were produced as follows. Firstly, a plastic film is prepared on a glass sheet by dispersing a drop of 0.25% Triafol in ethyl acetate with 1 % glycerine. The formed film is removed to water by immersing the glass in it and is then attached on a metal grid of 3.05 mm diameter with 400 mesh (Ni, Cu, Mo and Au grids

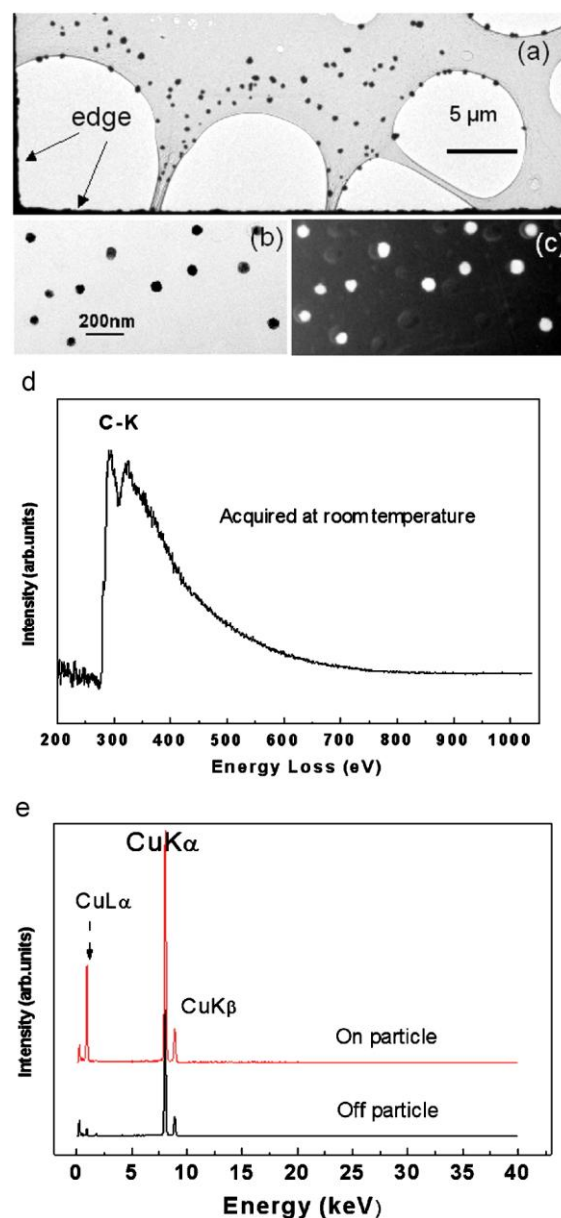


Fig. 1: (a) An overview TEM image of α -C film supported on Cu grid after *in-situ* heating at 600 °C for 0.2 h and at 660 °C for 2.5 h; Cu nano-particles are randomly distributed on α -C film; (b) and (c) are bright-field image and high-angle centred dark-field image, respectively; (d) is an spliced EELS spectrum measured from α -C film prior to heating. Note that no Cu signals are detected at about 923 eV. (e) EDXS spectra measured on and off particles show the difference in Cu *La* line intensity; no other elements are detected.

are available from PLANO GmbH). The grid bars are (14.60 ± 0.10) μm, and the square mesh sizes are (45.70 ± 0.15) μm. In a next step the metal grids covered with plastic film is coated with a carbon film by evaporation (ac-discharge of graphite rods in vacuum). Submerging the covered grids in ethyl acetate for a sufficient time removes the plastic film completely and leaves just an amorphous carbon film on metal support. The α -C films were made in the same way on all metal grids (Ni, Cu, Mo and Au).

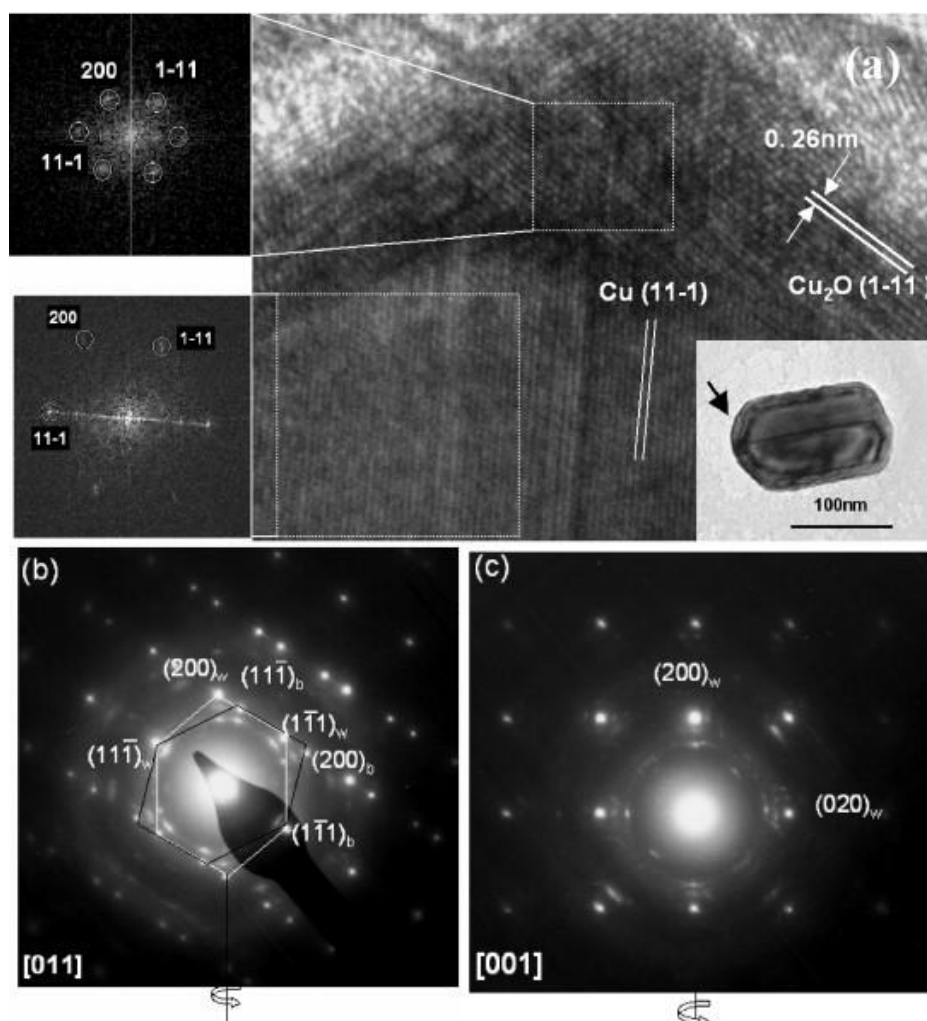


Fig. 2: (a) An enlarged HRTEM image of one Cu nano-particle with core-shell structure (the bright field image and the FFTs of the part of the shell and Cu core in the high-resolution image are inserted; the arrow in the bright field image indicates the area where the HRTEM is recorded). Tilting series of electron diffraction taken on the particle are shown in (b) and (c). The diffraction spots correspond to the patterns of Cu [011] and [001] zone, where the diffraction rings result from Cu_2O oxide shell. The twin structure in (b) is denoted by two sets of hexagonal patterns with black (labelled by *b*) and white (labelled by *w*) lines.

3. Experimental observations

3.1. Cu grid coated with α -C film

The Cu grid is coated with a very thin and holey C film. The film thickness relative to the total inelastic mean free path is about 0.1. (The relative sample thickness is defined by the ratio of thickness (*t*) to total inelastic mean free path (λ) of electron, t/λ [13]). The carbon film is amorphous and quite clean, which is verified by SAD/TEM and by EDXS/EELS on different parts of as-prepared thin holey C film over large areas about a few microns in diameter. *In-situ* heating experiments reveal that Cu nano-particles are formed at 600°C after heating for a short period whereas larger Cu nano-particles occur immediately at 700°C. Prolonged heating up to 2.5 h at this temperature results in many larger Cu nano-particles randomly distributed on α -C film.

Fig.1 displays a low magnification electron micrograph of a holey α -C film covering one half mesh of the Cu grid with (Fig. 1a), taken after heating the grid at 720°C for 1h 45 min. The bright-field (BF) image and corresponding conical dark-field image [14] are shown in Figs. 1b and 1c, respectively. These images prove that particles of tens of nano-meters in size are formed during heating the bare Cu-grid in microscope. Fig.1d is a spliced EELS spectrum measured from α -C film prior to heating, where no Cu signals appear at energy position of 923 eV. EDXS spectra (Fig.1e) measured on and off one Cu particle show the slight difference in Cu $L\alpha$ line intensity although most contribution of Cu signals results from the excitation of Cu grid bars, however, both indicate that only Cu presences. Taken together, these results prove that Cu nanoparticles are present after heating, and that no other elements are found.

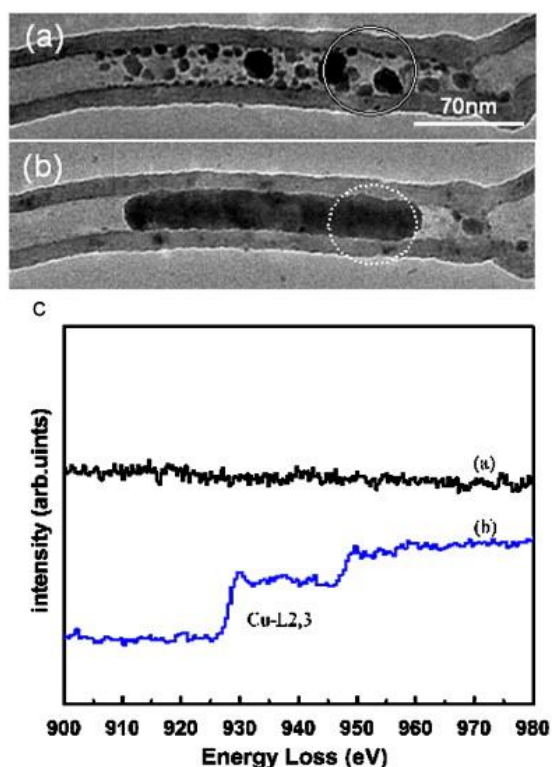


Fig. 3: BF images of a carbon nanotube containing Pt particles before (a) and after heating at 600°C for 8 hours (b). Cu atoms diffuse into carbon nanotube filled with Pt particles forming a nanorod inside the tube. (c) Comparative EELS spectra taken on the area indicated in (a) and (b). EELS spectrum from (b) shows Cu-L edge at about 923 eV in the Pt-Cu alloy nano-rod. Note that the entire volume of material in the tube is obviously increased after heating.

Ensuig HRTEM and electron diffraction studies (Figs.2) reveal that these nano-particles are Cu particles. BF image (inset in Fig. 2a showing the overview image of one particle and the location where HRTEM image was taken) and high-resolution image (FFTs inserted) show that the particles are covered with a thin Cu oxide overlayer formed during the mount of Cu-grid from heating holder to normal TEM holder for EDXS measurement. The Cu oxide overlayer occurs only when Cu nano-particles are exposed to air, and disappears when annealed again in TEM column. Lattice spacings in Fig 2 match well those of Cu oxide (Cu_2O) and those of *fcc* Cu structures. Tilting series of diffraction patterns along $[-200]$ zone taken from an isolated nano-particle are illustrated in Figs.2b and 2c. The crystallographic analysis indicates that the patterns are from *fcc* Cu of $[001]$ and $[011]$ zones, respectively. The rings are assigned to those of Cu_2O thus confirming the presence of copper oxide. Diffraction pattern in Fig.2b reveals the orientation relationships of two parts in the twinned particle

The high thermal variability (instability) of such Cu grids coated with α -C film can induce unexpected effects when used *in-situ* heating experiments. For example, in a study of the dynamic confinement effect of carbon nano-

tube containing Pt nano-particles, we found that Cu atoms diffuse into the Pt filled carbon nanotubes through the open end and form nanorods of Pt-Cu alloy inside the carbon nanotube during annealing for 8 hours at 600°C (Fig.3). Consequently, the volume of material within the tube is obviously expanded as compared with the tube prior to heating.

3.2. Cu grid coated with silicon monoxide film

The Cu grid is coated with a thin amorphous silicon monoxide film (SiO , from PLANO GmbH, D-35578 Wetzlar) of relative thickness 0.1~0.14. A typical low-magnification TEM image prior to heating, together with a representative EDXS spectrum measured on the location close to Cu grid bar, are shown in Fig.4a and Fig.4c (the red spectrum), separately. Apparently, the film is of homogeneous composition over a large region before heating except that Ta signals originated from heating holder. The grid was subsequently subjected to heating treatment at 550°C for 0.5 h, 700°C for 3.5 h, and then at 820°C for 20 minutes in TEM. After the heating experiment the BF image (Fig. 4b) reveals that no nano-particles are formed and EDXS measurement within several meshes close to Cu grid bars (Fig.4c, the black spectrum) shows no detectable change in the film composition, which means the carbon film is homogenous. A typical HRTEM image (FFT inset) before heating is shown in Fig.4d. EELS spectra from SiO film at 820°C (Fig.4e), recorded about several microns away from grid bar, illustrate the fine structure of Si-L, O-K edge, and noticeable intensity from C-K edge. This signifies that Cu-grid with SiO film is stable at a temperature up to 820°C, provided the illuminating electron dose is low. EELS spectra from the other meshes at the positions near to grid bar and to the centre give the same results.

However, we found that the stability of SiO film can be changed if it is exposed to intense electron beam at high temperature. Once high electron beam density is used, for instance, and high-resolution image is recorded at 700°C, the silicon monoxide film is unstable, numerous single and multiple-twinned nano-particles are invariably formed in the SiO film (see Fig.5). Two consecutive HRTEM images (Figs.5a and 5b) show that under this illumination condition (current density of about $10\text{-}20\text{A}/\text{mm}^2$) nano-crystals emerge from the amorphous film within 10 min at 700°C. This can be seen in the diffractogram in Fig.5b as well, where additional dots appear. HRTEM analysis indicates that the formed nanoparticles are Si particles, and the fringe spacings both in Fig.5b and Fig.5c correspond to Si (111) plane with a spacing of 0.312 nm. Detailed EELS analysis (Fig.5c and 5d) performed on Si nano-particle with twin boundaries reveals the distinct differences between the as-deposited SiO film and the Si nano-crystal, especially in the fine structure of Si-L_{2,3} edge. In contrast to the as-deposited SiO film, Si-L_{2,3} edge onset from nano-particle shift to low energy position at about 99 eV and a very small

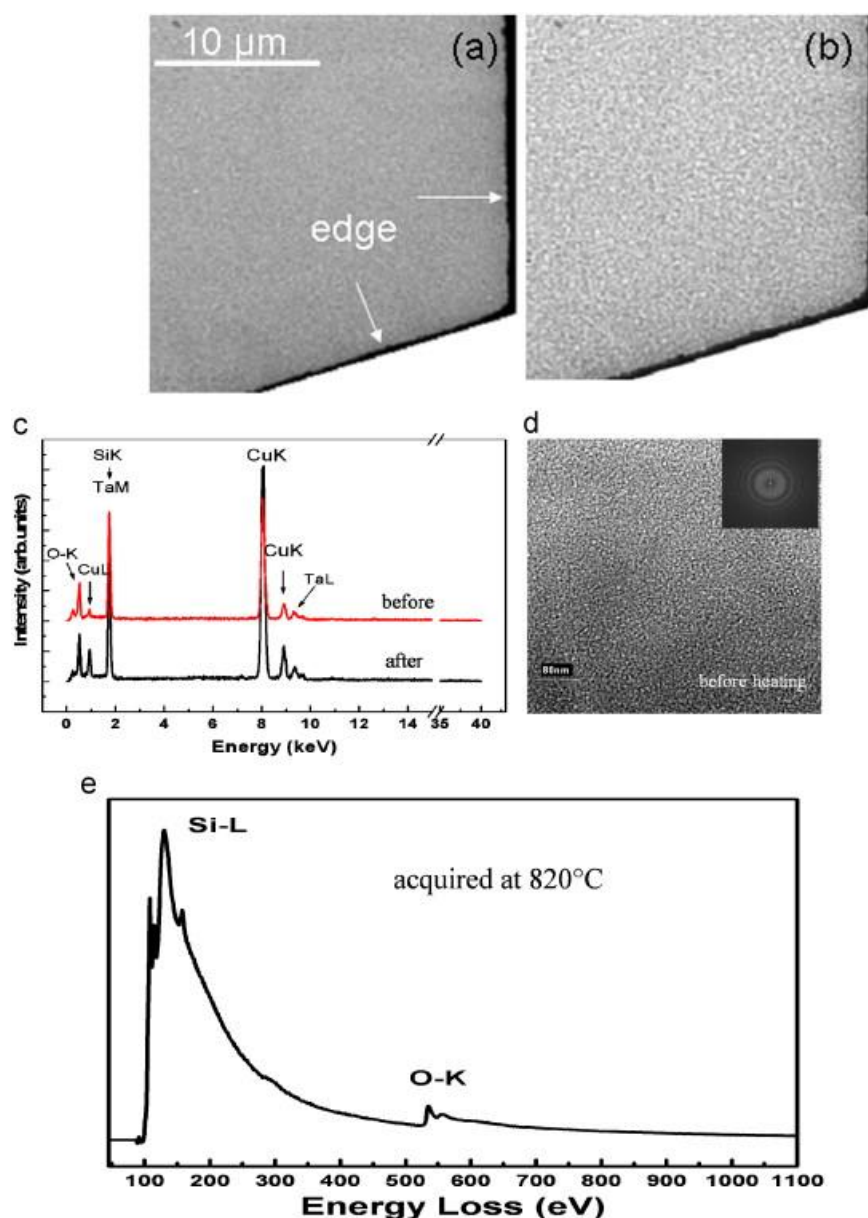


Fig. 4: (a) and (b) typical low-magnification TEM images of SiO film supported on Cu-grid prior to and after heating, (c) EDXS spectra measured on a location close to Cu grid bar (the upper red and lower blue spectrum are from before and after heating, respectively). Note that Ta peaks originate from heating holder. (d) HRTEM image (FFT inserted) of SiO film before heating. The grid was subjected to heating treatment at 550°C for 0.5 h, at 700°C for 3.5 h, and finally at 820°C for 20 min. (e) EELS spectrum acquired from SiO film at 820°C, showing Si and O signals as well as signals from C. No Cu signal is detected.

peak at 100.8 eV emerges which corresponds to Si $L_{2,3}$ in Si bulk.

3.3. Ni grid coated with α -C film

Ni grid coated with α -C film is often used for *in-situ* heating experiments [9]. One Ni grid coated with α -C film (relative thickness is about 0.13, EDXS spectrum shows that α -C film is homogeneous in composition) was heated up to 600°C for 1.3 hour, 700°C for 0.5 hour, then 750°C for 1.0 hour and finally to 800°C for 0.3 hour. A series of

bright field images (Figs.6a-d) show that Ni nano-particles appear on the support film at the edge of one mesh. At 600°C, only a few Ni nano-particles (Fig.6b, indicated by arrow) were observed near the edge of the mesh whereas considerable amount of Ni nano-particles emerge after heated at 700 and 800°C (Fig.6c and 6d). Note that the nano-particles at first near the edge of grid bar, and spread toward the central part of a mesh through Ni atom diffusion on the carbon film with the prolonged annealing time and increasing temperature. Fig. 6e is an enlarged BF image taken in one region containing one larger and a certain amount of small particles and the corresponding diffraction

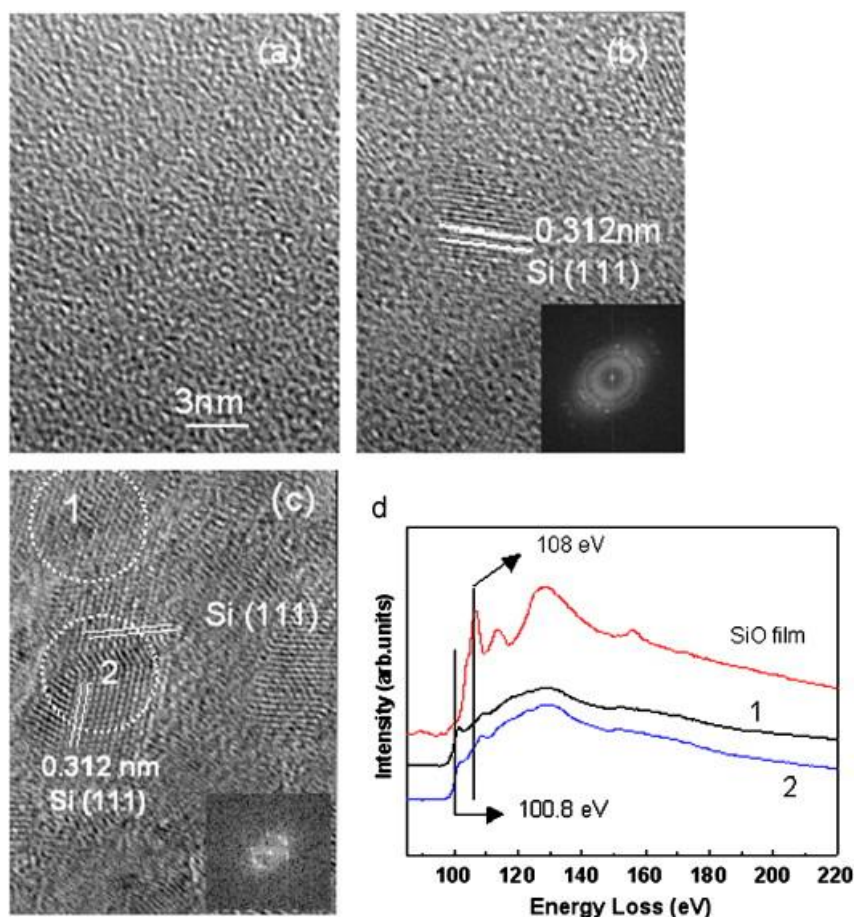


Fig. 5: Evolution of the structure of SiO film supported on Cu grid at 700°C: (a) at the beginning and (b) at 10 min when Si particles occur. (c) HRTEM image of twinned Si particles; (d) EELS spectra taken at different areas in (c) and done from a SiO film, revealing Si $-L_{2,3}$ fine structure variations in Si nanoparticle and twinned Si nanoparticle as well as in SiO film.

pattern is inserted in the left low corner. Electron diffraction, together with HRTEM and EELS analysis, reveals that the formed particles during heating are pure Ni. The spots in diffraction pattern are from a large Ni particle along $[-112]$ zone axis, while the rings from numerous tiny Ni nanocrystalline indexed as Ni (111) and (220) reflections. In contrast to the nano-particles on a Cu grid, Ni nanoparticles are quite inhomogeneous in size. A typical HRTEM image of particle with Ni-L ELNES is shown in Fig. 6f, and plane spacings corresponds to Ni (111) plane. Nearly all Ni nano-crystals are wrapped by graphite sheet. This is due to the in- and out-diffusion of carbon atoms on Ni nano-crystal surface at the high temperature, a phenomenon similar to those in the synthesis of carbon nanotubes where Ni acts as a catalyst for hydrocarbon decomposition and as seed for the growth of carbon nano-tube by diffusion of atomic carbon on the Ni particle surface [15]. No carbon nanotubes are formed due to the limited diffusion rate in our case (no gas-phase carbon sources available). EELS spectra recorded from graphite in the nanocrystalline regions and as-deposited α -C film are illustrated in Fig. 6e, showing characteristic of C-K fine structure of amorphous and graphite carbon.

3.4. Mo grid coated with α -C film

Mo grid is an alternative TEM grid used for experiment at elevated temperature. Blank testing experiment of Mo grid coated with α -C film (relative thickness 0.1~0.16) demonstrates that such grid is stable at temperatures up to 800°C. Typical TEM images of homogeneous α -C film are shown in Figs. 7a and 7b (FFT is inserted). EDXS measurement (Fig. 7c) reveals a homogenous film with uniform composition (Ta and Mo signals arise from the holder and grid, respectively.) over a large area. After heated at 580°C for 10 hours, and then 680°C for 1.5 hours, no nanoparticles in α -C film are detected, as shown in Fig. 7b.

3.5. Au grid coated with α -C film

Au grid is quite stable at elevated temperature and no particles are detected during *in-situ* heating up to 850°C by TEM. The heating is performed consecutively, at 600°C for 1 hour, at 700°C for 1 hour, at 800°C for 1 hour and at 850°C for 0.5 hour. The overview images in Figs. 8 near the edge of one mesh indicates that there is no changes of the

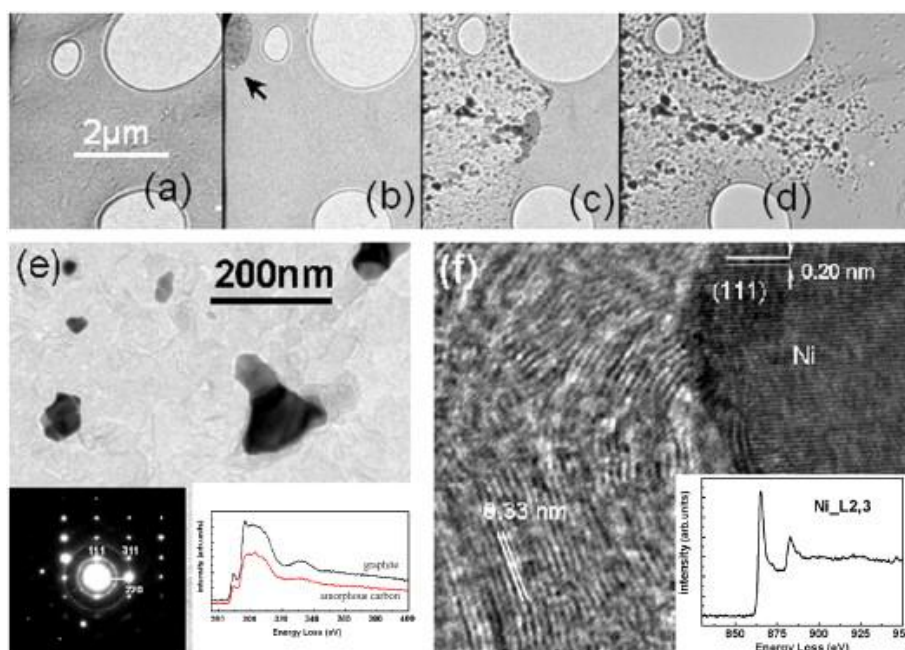


Fig. 6: A series of images showing the formation of Ni particles on α -C film supported on Ni grid during consecutively *in-situ* heating: (a) before heating, (b) at 600°C for 1.0 h, (c) at 600°C for 0.3 h more and at 700°C for 1.3 h, (d) at 750°C for 1.0 h and at 800°C for 0.3 h. (e) enlarged BF image and corresponding electron diffraction pattern and EELS spectra recorded from α -C film and graphite, respectively. (f) typical HRTEM image of Ni particles (Ni EELS spectrum is inserted as well) wrapped by several graphite layers.

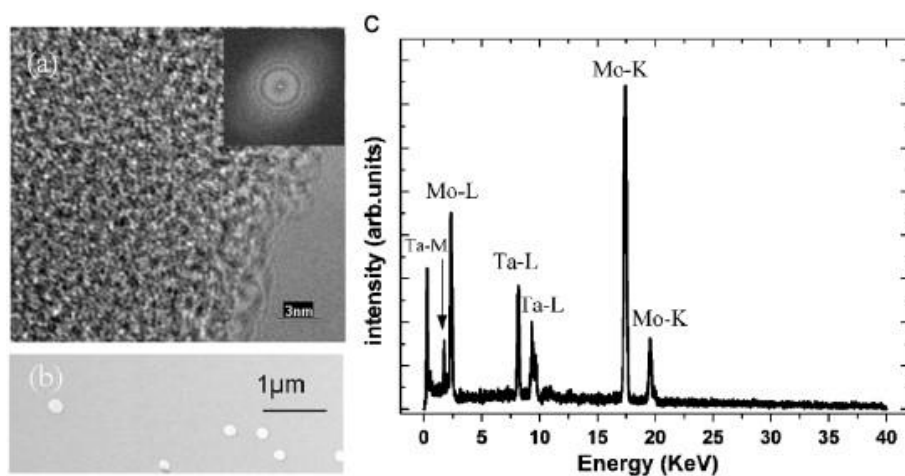


Fig. 7: (a) HRTEM image (FFT inserted) of α -C film supported on a Mo grid before heating; (b) a low magnification bright field image of α -C film after heating at first at 580 °C for 10 h and then at 680 °C for 1.5 h; (c), EDXS spectra measured from α -C thin film before heating, Ta and Mo signals are from the heating holder used and Mo grid, respectively.

Metal grid ^a	Exp. temp.	Particle	Remarks
Cu+ α -C film	600 °C 0.2 h+660 °C 2.5 h	Cu particles	580 °C for 2 h, stable; strongly temp. dependent
Cu+SiO film ^a	550 °C 0.5 h+700 °C 2 h+820 °C 0.3 h	Si particles	At room temp.+e beam, stable; At 550 °C+under e beam, particles occur, dose dependent.
Ni+ α -C film	600 °C 1.3 h+700 °C 0.5 h+750 °C 1 h+800 °C 0.3 h	Ni particles; graphite	Temp. dependent; 500 °C for 2 h, stable; up to 600 °C, Ni particles occur
Mo+ α -C film	580 °C 10 h+680 °C 1.5 h	Not detected	Up to 680 °C, stable
Au+ α -C film	600 °C 1 h+700 °C 1 h+800 °C 1 h+850 °C 0.5 h	Not detected	Up to 850 °C, stable

Table 1: Summary of the stability of metal grids during *in-situ* heating

^aCu grid coated with SiO film is available from PLANO GmbH; Cu grid coated with α -C film was homemade. *e* is an abbreviation for electron, Exp. is an abbreviation for experimental, Temp. is an abbreviation for temperature;

carbon film after the grid is subjected to heat treatment. This is further proved by EDXS spectra measured over an area about 1 micron in diameter (Fig.8c), and for comparison, one typical spectrum acquired prior to heating is included as well.

In summary, the metal grids coated with α -C film or Si monoxide films demonstrate distinct stabilities during *in-situ* heating. Under present experimental conditions (Table 1), metal nano-particles may form when Cu and Ni grids are used while no metal particles are detected as heating Mo and Au grids. In case of Cu grid covered with SiO film, the film is electron beam sensitive and Si nanocrystals may occur. For comparison, the experimental results are tabulated below (Table 1).

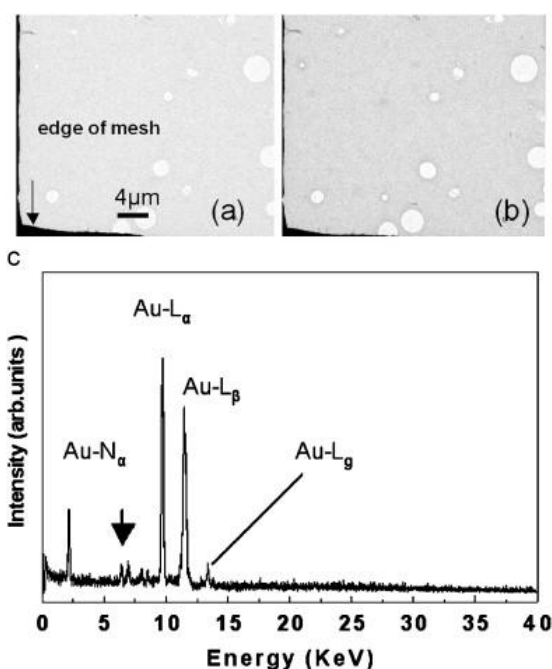


Fig. 8: The BF image of Au grid coated with α -C before (a), and after *in-situ* heating (consecutively for 1 h at 600°C, 700 °C and 800°C, and then for 0.5 h at 850 °C) (b). No particles are observed. (c) EDXS spectra acquired from α -C film prior to and after heating.

4. Discussion

In a clean TEM-column, free of contamination, two general processes may occur on the specimen support during *in-situ* heating: 1). Sublimation of metal depending on its melting temperature; 2). Interaction of metal grid with supporting films. The two processes could be simultaneous at elevated temperature, but only one process may be dominant, depending on the nature of metal grid.

Fig.9 shows the variation of the metal vapour pressure of the four metals with temperature. From the viewpoint of sublimation, under the identical conditions Cu exhibits a relatively high vapour pressure compared with Au, Ni and Mo so that Cu is more likely to form vapour

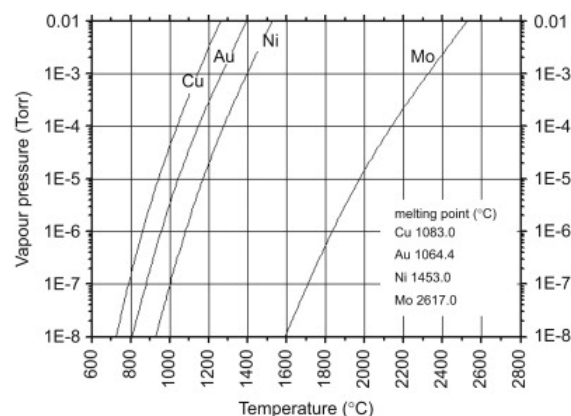


Fig. 9: Dependence of vapour pressure of Cu, Au, Ni and Mo on temperatures.

droplet at elevated temperature [11], especially as the temperature approach to melting point (\sim 1083°C). The heating experiments on metal grids coated with amorphous film largely prove different evaporation behaviours, for instance, Cu nano particles occur grid when temperature approach to 600°C for long holding or immediately appear after 700° C due to a high vapour pressure, whereas no Au nano particles form at 700°C.

On the other hand, the interaction of metal grid with supporting film plays an essential role in the formation and growth of metal nano particle. By means of an extended analysis, i.e. phase transformation, diffusion, the likely interactions between various grids and supporting film are addressed as follows.

For the Cu grid coated with α -C film, there is no Cu carbide phase reported. The solubility of C in solid Cu is extremely low. However, Cu atom exhibiting high mobility can diffuse rapidly on the surface of α -C and graphite, i.e. under intensive electron beam irradiation [16] and heating [11]. This high mobility can result in the formation of Cu nano-rods and nano-wires on the edge of holey α -C film. Considering the energy barriers of atom mobility, we believe that the movement of Cu follows by surface diffusion. Surface diffusion of Cu does not happen on amorphous carbon at room temperature [17], but any activation, for instance heating, may result in overcoming the diffusion barriers. It is thus reasonable to believe that surface diffusion is enhanced during *in-situ* heating at high temperature, which is responsible for the formation of Cu nano-particles. However, when the heating temperature is sufficiently high, i.e approaching to 800°C, the atom diffusion is strengthened to a large extent, and the possibility to form Cu droplet is enormously enhanced as well. Consequently, Cu particles can occur immediately once a higher temperature is arrived, and a quick growth of particle/ nano-rod by Ostwald ripening on α -C film is followed in a short holding period [11].

The formation of Cu particles under *in-situ* condition is obviously affected by the support film. In contrast to Cu grid coated with α -C film, no Cu particles are formed when

Cu-grid is coated by SiO film. It seems that the mobility of Cu on SiO film is suppressed dramatically due to the strong reaction of Cu with SiO film [18], which results in the formation of Cu-rich silicides as shown in Cu/SiO/Si system [18]. At elevated temperature, Cu oxide can also be formed [19-20] as demonstrated in deficient γ -Al₂O₃ substrate [21]. Both processes suppress Cu mobility in SiO film. However, under *in-situ* heating condition SiO film can be easily reduced by a strong electron beam illumination leading the formation of twinned Si nano-particles [22-24]. It should be mentioned that at room temperature silicon monoxide is hardly decomposed even if a high electron beam density is used.

In the experimental temperature ranges the vapour pressure is low that Ni nano-particles are unlikely to be formed through either Ni vapour or rapid Ni diffusion at a relatively low temperature. According to phase diagram, Ni and C can form carbide at about 300°C [25-26], but such Ni carbide is meta-stable and rapidly decomposed at higher temperature [26]. At the temperature (600°C or higher) used in our experiment, Ni diffusion in α -C film plays a dominant role in the formation of Ni nanocrystal. Ni atom directly diffuses onto α -C film from the grid, aggregate and nucleates, leading to the formation and subsequently growth of Ni nanocrystals. The diffusion rate of Ni on α -C film is largely enhanced by increasing temperature. Therefore, more Ni nanocrystals and some larger Ni particles occur in α -C film with temperature increasing (see Fig.6c and 6d). Once the Ni nanocrystals form, they catalyze the amorphous carbon transforming into graphite sheets as is shown in Fig.6.

While molybdenum and carbon can form stable carbides at elevated temperature Au and carbon can not, although it is reported that an interaction layer may exist between Au and carbon [27]. Under the identical conditions Au vapour pressure is high compared with Mo (Fig.9), but both are lower than Cu. This is the reason why Au and Mo can hardly form vapour droplet at experimental temperature (lower than 850°C) in TEM. From the viewpoint of diffusion, Au can diffuse in α -C film even at room temperature forming Au islands after *months* of storage [28], but it is apparently not as rapid as the diffusions of Cu on α -C film. It has to be pointed out however that although there is no Au nano-particle being detected in Figs.8, extremely small and rather fewer amounts of Au nano-particles may form during heating, which is beyond the detecting limit of normal microscope [29].

As discussed above, two factors, the interaction of metal grid with supporting film and the vapour pressure of metal, play key roles in determining the emergence of nano-particles during *in-situ* heating. The strength of interaction with α -C film increases in the sequence of Cu, Au, Ni, and Mo, whereas the vapour pressure decreases in this sequence. Strong interaction of metal with covering film

can suppress the diffusion of metal in the film, while low vapour pressure can considerably lower the probability for the formation of metal droplets. It is therefore reasonable to conclude that Mo grid covered with α -C film seems particularly suitable for *in-situ* TEM heating experiments, and an alternative is Au grid when the heating temperature is lower than 850°C.

It is necessary to mention that the residual gas in TEM column may play a role during heating. So far, however, no detailed study has been performed about the role of such gas on experimental observation. Chemically, it cannot completely eliminate such effect, particularly during *in-situ* heating. The main issue is how strong such effect could be if it is present. However, experiments found no detectable differences about the influences of residual gas from two different TEMs on the condensation behaviours of the metals on α -C [29]. Experimentally, precaution is definitely necessary during *in-situ* TEM. Often cleaning, for instance, the Hexring, washers, and heating holder by plasma, are always essential as they could be heavily contaminated by the preceding experiments.

5. Summary

The thermal stability of several typical TEM metal grids was closely examined as they are often employed during *in-situ* heating experiments in microscope. It is clearly shown that some grids possibly produce side effects, e.g., generate nano-crystals at elevated temperature, which can mislead interpretations of experimental results. These are particularly demonstrated on Cu and Ni grid covered with α -C film. The commonly used Cu grid is unstable as numerous copper nano-particles can form at temperatures higher than 600°C. The Cu nano-particles can even migrate into carbon nanotube at elevated temperature due to its high diffusivity on α -C film. As to the Cu grid covered with thin amorphous SiO film, they are thermally stable, but the SiO film can decompose under an intensive electron beam when heated up to a high temperature. In the case of Ni grid covered with α -C, a large number of Ni nano-crystals are observed, accompanied by the graphitization of amorphous carbon. In contrast, both Mo and Au grids covered with α -C film exhibit good stability at elevated temperature (at least $\leq 600^\circ\text{C}$) and do not produce any nano-particles.

Acknowledgement

Thanks are due to Mr. H. Sauer for his helpful discussions and to Professor R. Schlögl and Professor E. Zeitler, Fritz-Haber Institute, Max-Planck Society, for critical reading of the manuscript.

References

- [1] L. D. Marks, Rep. Prog. Phys. 57(1994)603.
- [2] Z. L. Wang, J. Phys. Chem. B104(2000) 1153.
- [3] P.A. Buffat, Phil. Trans. R. Soc. Lond. A361(2003) 291.
- [4] Y. Wu, P. Yang, Adv. Mater.13(2001) 520.
- [5] Z.L.Wang, J.M. Petroski, T. C. Green, M.A. El-Sayed, J. Phys. Chem. B102 (1998) 6145.
- [6] R.Yu. H.Song, X.-F.Zhang, P. Yang, J. Phys. Chem. B 109(2005)6940.
- [7] M. Jose-Yacamán, C. Gutierrez-Wing, M. Miki, D.-Q. Yang, K. N. Piyakis, E. Sacher, J. Phys. Chem. B109(2005) 9703.
- [8] H.Suzuki, M. Shintaku, T. Sato, M.Tamano, T.Matsuura, M.Hori, C.Kaito, Jpn. J. Appl. Phys., 44(2005) L610.
- [9] I. Lisiecki, H. Sack-Kongehl, K. Weiss, J. Urban, M.-P. Pileni, Langmuir, 16(2000) 8802.
- [10] R.J.Liu, P.A.Crozier, C.M.Smith, D.A.Hucul, J.Blackson, G.Salaita, Microsc.Microanal. 10(2004)77.
- [11] Z.W.Liu, Y.Bando, Adv.Mater. 15(2003) 303.
- [12] K. Chatterjee, J.M. Howe, W.C. Johnson, M. Murayama, Acta Materialia. 52 (2004) 2923.
- [13] M.M.Disko, C.C.Ahn, B.Fultz, eds. (1992), P47, *Transmission electron energy loss spectrometry in materials science*, The Minerals, Metals and Materials Society, Warrendale, Pennsylvania
- [14] U. Kaiser, A. Chuvilin, Microsc.Microanal. 9(2003)36.
- [15] S. Helveg, C.Lopez-Cartes, J. Sehested, P. L. Hansen, B.S. Clausen, Jens R. Rostrup-Nielsen, F. Abild-Pedersen, J. K. Nørskov, Nature, 427(2004)426.
- [16] P.-I Wang, Y.-P Zhao, G.-C.Wang, T.-M. Lu, Nanotechnology 15 (2004) 218.
- [17] W.F. Egelhoff, Jr., G.G.Tibbetts, Phys. Rev. B 19(1979)5028.
- [18] N. Benouattas, A. Mosser, D. Raiser, J. Faerber, A. Bouabellou, Applied Surface Science 153(2000)79.
- [19] Y. Ito, H. Jain, D. B. Williams, App.Phys.Lett. 75(1999)3793.
- [20] H. Amekura, K. Kono, Y. Takeda, N. Kishimoto, Appl.Phys.Lett., 87(2005) 153105.
- [21] K.Sun, J. Liu, N.D. Browning, Applied Catalysis B: Environmental 38 (2002) 271.
- [22] M.Takeguchi, K. Furuya, K. Yoshihara, Micron 30 (1999) 147.
- [23] Y. Q. Wang, R. Smirani, G. G. Ross, F. Schiettekatte, Phys.Rev. B 71(2005)161310.
- [24] X.-W. Du, B. Wang, N.Q. Zhao, K. Furuya, Scripta Materialia 53 (2005) 899.
- [25] S. Nagakura, J Phys Soc Jpn.,12 (1957) 482.
- [26] R.Sinclair, T.Itoh, R.Chin, Microsc.Microanal., 8 (2002)288.
- [27] S. Arcidiacono, J. H. Walther, D. Poulidakos, D. Passerone, P. Koumoutsakos, Phys. Rev.Lett., 94(2005)105502.
- [28] R.Werner, M.Wanner, G. Schneider, D. Gerthsen, Phys. Rev. B72 (2005)045426.
- [29] A.A. Schmidt, H. Eggers, K. Herwig, R. Anton, Surface Science 349 (1996) 301 316.